

RESEARCH

Open Access



PbrBGAL6 promotes pollen tube growth by influencing apical pectin level in *Pyrus bretschneideri*

Yusheng Xu¹, Lan Xu¹, Mingliang Zhang², Hao Wang¹, Yuqian Wang¹, Xueping Zhang¹, Kaijing Zhang¹, Yihu Sui¹, Jingjing Qian¹, Shuangshuang Jia¹, Ming Qian^{1*} and Guangrong Cui^{1*}

Abstract

Background β -galactosidase (BGAL), which is an important cell wall-degrading enzyme, participates in various biological processes, but its effects on pollen tube growth (PTG) remain unclear.

Results We identified 12 *PbrBGAL* genes (named *PbrBGAL1–12*) in the pear (*Pyrus bretschneideri*) genome. *PbrBGAL* members, containing three conserved domains and two enzyme active sites, were grouped into six subclasses. They were distributed in seven chromosomes, with dispersed duplication revealed as the main replication event. *PbrBGAL* genes contained 1 to 24 exons and 0 to 23 introns, with exon/intron structure mostly conserved within each subclass except for subclass E. Analyses of tissue-specific expression indicated that only *PbrBGAL6* was highly expressed specifically in anther and pollen, with decreasing expression levels during PTG. The effective inhibition of *PbrBGAL6* expression using antisense oligodeoxynucleotide technology dramatically decreased BGAL enzymatic activity, promoted PTG and increased cytoplasmic leakage and tip widths. Furthermore, suppressing *PbrBGAL6* transcription decreased the apical total and methylated pectin contents in pollen tubes by significantly increasing transcription of *PbrPME11*, *PbrPG14*, *PbrPG20*, *PbrPG21* and *PbrPG24*.

Conclusions We identified 12 *PbrBGAL* genes in the pear genome, of which *PbrBGAL6* precisely modulates the apical pectin content to mediate pear PTG through its effects on *PbrPME11* and *PbrPGs* expression. This study provides direct evidence of the involvement of BGAL in the regulation of polar PTG.

Keywords Pear, β -galactosidase, Pollen tube growth, Cell wall, Pectin, Gene family

Background

In flowering plants, self-incompatibility (SI), which is a common mechanism detected in more than 100 families, is controlled by multiple genes that prevent inbreeding depression and promote hybrid vigor, thereby maintaining plant diversity [1]. However, to optimize yield during crop production, SI is overcome via artificial pollination, but this leads to increased costs, especially for pear (*Rosaceae*) fruit production. Pear has a typical gametophyte SI mechanism in which pistil S-RNase triggers toxic cascade signals that inhibit the pathway necessary for pollen tube growth (PTG), leading to programmed pollen tube cell death and a

*Correspondence:

Ming Qian
m13637099856@163.com
Guangrong Cui
cuigr64@sina.com

¹ Department of Horticulture, College of Agriculture, Anhui Science and Technology University, Chuzhou 233100, China

² College of Horticulture, Nanjing Agricultural University, Nanjing 210032, China



© The Author(s) 2025. **Open Access** This article is licensed under a Creative Commons Attribution-NonCommercial-NoDerivatives 4.0 International License, which permits any non-commercial use, sharing, distribution and reproduction in any medium or format, as long as you give appropriate credit to the original author(s) and the source, provide a link to the Creative Commons licence, and indicate if you modified the licensed material. You do not have permission under this licence to share adapted material derived from this article or parts of it. The images or other third party material in this article are included in the article's Creative Commons licence, unless indicated otherwise in a credit line to the material. If material is not included in the article's Creative Commons licence and your intended use is not permitted by statutory regulation or exceeds the permitted use, you will need to obtain permission directly from the copyright holder. To view a copy of this licence, visit <http://creativecommons.org/licenses/by-nc-nd/4.0/>.

lack of double fertilization [2]. Therefore, revealing the PTG mechanism may be useful for breaking pear SI to generate high-quality self-compatible germplasm.

PTG involves various processes, including cell wall remodeling and deposition, concentration gradient (ROS, pH, and Ca^{2+}) formation and maintenance, actin cytoskeleton organization and activity, hormone homeostasis, and orderly vesicular trafficking [3]. Among these processes, regulated changes to the cell wall are crucial for maintaining cell wall integrity, which influences PTG [4]. The pollen tube wall primarily consists of methylated pectin ('soft pectin') secreted by vesicles in the tip region. Additionally, the shank region contains demethylated pectin ('hard pectin'), callose, cellulose, and hemicellulose synthesized by related enzyme complexes. [4–6]. Previous studies showed that the composition and contents of these cell wall polysaccharides are regulated by various related enzymes that mediate cell wall remodeling and deposition to control PTG, including callose synthase in pear [7] and *Arabidopsis thaliana* [8], cellulose synthase in pear [9] and tobacco [10], and β -glucanase in lily [11] and peach [12]. Notably, pectin, which is a complex cell wall polysaccharide comprising three main supramolecular domains (homogalacturonan (HG), rhamnoglacturonan I (RG-I), rhamnoglacturonan II (RG-II)) synthesized in Golgi bodies and transported by secretory vesicles [13–15], is critical for the precise regulation of structural and mechanical properties during polarized PTG [16]. Additionally, during PTG, HG domain in Golgi bodies is methylated at the C-6 carboxyl group by pectin methyltransferase and exported to the tip, after which they are cross-linked with Ca^{2+} in the cell wall following a reaction catalyzed by tip-localized pectin methyltransferase (PME; EC 3.1.1.11) to form demethylated pectin. This establishes an apical concentration gradient of methylated pectin (i.e., highest methylated pectin level at the tip) that facilitates tip growth, while also increasing shank strength [5, 17, 18]. Meanwhile, polygalacturonase (PG; *endo*-PG: EC3.2.1.15, *exo*-PG: EC3.2.1.67) degrades the demethylated HG domain by specifically hydrolyzing the α -(1–4) glycosidic bond to precisely modulate the pectin level [19, 20]. Adjustments to the HG domain esterification state and level requires the coordinated regulation of other enzymes or inhibitors, including pectin acetyltransferase (PAE; EC 3.1.1.6), pectate lyases (PL; *endo*-PLs: EC4.2.2.2, *exo*-PLs: EC4.2.2.9), pectin lyases (PNL; EC4.2.2.10) [19], and the PME inhibitor [21]. Earlier research on the regulatory effects of pectin on PTG mainly focused on HG-modifying enzymes, with relatively few reports on the rhamnoglacturonan (RG) domain.

RG-I is a heteropolymer composed of alternating α -1,4-linked GalA residues and α -1,2-linked rhamnose that combine primarily with 1,4- β -D-galactose or 1,5- α -L-arabinose residues to form neutral side-chains. RG-II has an HG backbone with side-chains containing various sugars [22]. A β -galactosidase (BGAL) belonging to the glycoside hydrolase 35 family, which is the only *exo*- β -galactosidase (EC3.2.1.23) in higher plants, catalyzes the removal of β -D-galactosyl residues from the side-chain non-reducing terminal of RG-I in pectin and hemicellulose. Specifically, BGAL is assumed to hydrolyze β -(1,4) (class I BGAL) as well as β -(1,3) and β -(1,6) (class II BGAL) glycosidic bonds to increase cell wall porosity, which enhances the binding of PME, PG, or other hydrolases to pectin to modulate various biological processes [23]. The class I BGAL reportedly influences the ripening and softening of diverse fruits, including peach [24], sweet cherry [25], kiwifruit [26], and mango [27]. Class II BGALs are involved in many developmental stages. For example, they affect hypocotyls and young leaves in radish [28], leaves in spinach [29], and roots in *A. thaliana* [30]. In addition to degrading pectin side-chains during the above-mentioned processes, BGALs can also regulate peach fruit softening by modifying PG and PME activities [24]. Hence, BGALs serve as enzymes and regulatory factors. However, the possibility BGALs regulate PTG remains unclear.

BGAL genes with unique consensus active site sequences (G-G-P-[LIVM](2)-x(2)-Q-x-E-N-E-[FY]) have been identified in *A. thaliana* (17) [31], *Oryza sativa* (15) [32], *Brassica campestris* (27) [33], *Ipomoea batatas* (17) [34], *Linum usitatissimum* (43) [35], *Gossypium hirsutum* (51) [36], *Cucumis melo* (21) [23], *Solanum lycopersicum* (17) [37], *Pyrus pyrifolia* (8) [38], *Persea americana* (4) [39], *Prunus persica* (17) [40], *Fragaria ananassa* (4) [41, 42], *Malus domestica* (13) [43], suggesting plant BGAL genes belong to a multigene family. On the basis of real-time quantitative PCR (qPCR) results, BGAL genes may be expressed in a tissue-specific manner. For example, in Japanese pear, *PpGAL1*, -2, -3, and -4 are expressed in fruits, whereas *PpGAL5*, -6, and -7 can be expressed in both fruits and leaves [38]. Similarly, in avocado, *AV-GAL1* is highly expressed exclusively in fruits, while *PaGAL2* and *PaGAL3* transcripts accumulate in both fruits and leaves [39]. In sweet potato, BGAL-encoding genes are mainly expressed in roots or stems, including *Ibbgal3*, -5, -6, and -10 in the young stem, *Ibbgal4* and *Ibbgal13* in the old stem, *Ibbgal8* in the fibrous root, and *Ibbgal11* in the storage root [34]. Interestingly, many BGAL genes are abundantly expressed in the floral organs of different plants, including *AtBGAL7*, -11, and -13 in *A. thaliana* [37], *OsBgal10* and *OsBgal11* in rice [32], *LuBGAL9*, -15, 16, -18, -21, and -39 in flax

[35], *GhBGAL7*, -18, -33, and -43 in cotton, *CmBGAL2*, -3, and -4 in melon [23], *Mdβ-Gal6*, -7, and -11 in apple [43], and *Faβgal1*, -2, -3 and -4 in strawberry [41, 42]. Furthermore, Liu et al. (2013) [33] determined that *BGAL* genes (*BcBGAL11*, -13, and -15) in Chinese cabbage are specifically expressed in pollen. Rogers et al. (2001) [44] reported that a tobacco *BGAL* (TP5) affects PTG because it is specifically produced in mature pollen grains [44]. These findings may reflect the functional diversity of *BGAL* genes, while also suggesting a possible link between *BGAL* genes and PTG. However, pear *BGAL* genes have not been identified and their expression patterns in tissues and roles during PTG are unknown.

In this study, we identified 12 *PbrBGAL* genes in the ‘Dangshansuli’ (*Pyrus bretschneideri* Rehder) genome and analyzed their chromosomal localization, conserved domains and active sites, structures, and evolutionary relationships using bioinformatics techniques. We revealed their expression patterns in 10 tissues and four pollen tube developmental stages on the basis of qPCR technology. Moreover, *PbrBGAL6* was identified as a major gene contributing to PTG using antisense oligodeoxynucleotide (as-ODN) technology. Finally, we

investigated whether *PbrBGAL6* affects apical methylated pectin by modulating *PME* and *PG* transcription. In summary, this study provides direct evidence of the regulatory effects of *BGAL* on PTG, with potential implications for optimizing the PTG mechanism.

Results

Identification of *PbrBGAL* family members in Chinese white pear

To clarify the role of *BGALs* during pear PTG, we first identified 12 *PbrBGAL* genes in the Chinese white pear genome; these genes were named *PbrBGAL1–12* (Table 1) according to their chromosomal positions. The predicted *PbrBGAL* sequences comprised 569–897 amino acids (aa), with a molecular weight of 64.26–99.56 kDa and an isoelectric point of 6.29–9.29. The *PbrBGAL2*, -3, -5, -6, -7, -8, -11, and -12 sequences included a signal peptide (Table 1). Four conserved domains were detected in *PbrBGAL2*, -3, -5, -6, -7, -8, -9, and -12, which was more than the three conserved domains in *PbrBGAL1*, -10, and -11 and the two conserved domains in *PbrBGAL4*. All *PbrBGALs* were

Table 1 Pear *BGAL* genes identified in this study

Gene Name	Gene ID	Description	Genome positions and direction	Deduced polypeptide				Domains ^d	Predicted localization
				Length (aa)	M _w ^b (kDa)	PI ^c	Signal Peptide		
<i>PbrBGAL1</i>	Pbr041454.1	Beta-galactosidase	Chr ^a 2: 18,663,762–18,668,311, -	670	75.06	7.54	-	1, 2, 3	Cell wall
<i>PbrBGAL2</i>	Pbr029017.1	Beta-galactosidase	Chr 3: 16,485,196–16,491,841, +	842	91.78	6.64	+	1, 2, 3, 4	Cell wall
<i>PbrBGAL3</i>	Pbr030918.1	Beta-galactosidase-like	Chr 4: 12,622,972–12,625,500, +	842	94.71	9.29	+	1, 2, 3, 4	Cell wall
<i>PbrBGAL4</i>	Pbr032491.3	Beta-galactosidase	Chr 9: 7,403,143–7,411,118, -	897	99.56	8.86	-	1, 2	Cytoplasm
<i>PbrBGAL5</i>	Pbr008870.1	Beta-galactosidase	Chr 9: 9,737,424–9,743,107, +	814	90.02	8.29	+	1, 2, 3, 4	Cell wall
<i>PbrBGAL6</i>	Pbr020737.1	Beta-galactosidase-like	Chr 10: 17,340,234–17,345,833, +	872	97.47	8.96	+	1, 2, 3, 4	Cell wall
<i>PbrBGAL7</i>	Pbr020639.1	Beta-galactosidase	Chr 11: 10,820,708–10,827,733, +	848	95.08	8.66	+	1, 2, 3, 4	Cell wall
<i>PbrBGAL8</i>	Pbr025610.1	Beta-galactosidase-like	Chr 11: 20,587,123–20,593,556, -	853	93.33	7.47	+	1, 2, 3, 4	Cell wall
<i>PbrBGAL9</i>	Pbr005903.1	Beta-galactosidase	Chr 15: 2,925,670–2,930,242, -	836	92.39	7.05	-	1, 2, 3, 4	Cell wall
<i>PbrBGAL10</i>	Pbr027955.1	Beta-galactosidase	Chr 15: 10,791,375–10,797,739, -	569	64.26	6.56	-	1, 2, 3	Cell wall
<i>PbrBGAL11</i>	Pbr015600.1	Beta-galactosidase	Chr 15: 14,970,907–14,975,799, -	731	80.94	6.29	+	1, 2, 3	Cell wall
<i>PbrBGAL12</i>	Pbr037415.1	Beta-galactosidase	Chr 15: 16,853,085–16,857,300, +	813	91.37	6.46	+	1, 2, 3, 4	Cell wall

^a Chromosome; ^bMolecular weight; ^cIsoelectric point;

^d 1: GH35 conserved sequence; 2: SCOP domain d1b9za2; 3: GHD domain; 4: Galactose binding lectin domain

predicted to be localized in the cell wall, except for *PbrBGAL4* in the cytoplasm (Table 1).

PbrBGAL sequence structure and conservation

PbrBGAL sequence characteristics were revealed by aligning sequences using DNAMAN software. According to the results and the classification by Eda et al. (2016) [45], *PbrBGAL* sequences can be divided into the following six regions: signal peptide region (*PbrBGAL6* as an example: 60 aa, M1–Q60), I (323 aa, V61–A383), II (58 aa, G384–S441), III (28 aa, Q442–E469), IV (167 aa, P470–G636), and C-terminal region (236 aa, L637–H872) (Fig. 1). Additionally, the *PbrBGAL* sequences contained three conserved domains (typical GH35 conserved sequence (G-G-P-[LIVM](2)-x(2)-Q-x-E-N-E-[FY]), SCOP domain d1b9za2, and GHD domain) and one relatively non-conserved domain (galactose-binding lectin domain) (Fig. 1). Moreover, all *PbrBGAL* sequences included two enzyme active sites (E217 and E288); however, three important functional sites (W/Y290, W/Q/F293, and V/Y/S/1600) differed among the examined sequences according to previous studies (Fig. 1) [45, 46].

Phylogenetic analysis of BGAL family members

A phylogenetic tree was constructed using the full-length BGAL protein sequences from 13 species. Twelve *PbrBGALs* were classified into six subclasses (A–C and E–G) according to the classification in *Cucumis melo* [23], with subclasses A (*PbrBGAL1*, –5, and –11) and E (*PbrBGAL3*, –6, –7, and –10) containing the most *PbrBGALs*. Subclasses B, C, F, and G contained one (*PbrBGAL9*), two (*PbrBGAL2* and *PbrBGAL8*), one (*PbrBGAL12*), and one (*PbrBGAL4*) *PbrBGALs*, respectively (Fig. 2). Most of the BGALs in the 13 selected species were classified in subclasses A, E, and F (especially subclasses A and E) (Fig. 2).

Genome distribution and structures of PbrBGAL genes in Chinese white pear

The 12 identified *PbrBGAL* genes were distributed on 7 of 17 Chinese white pear chromosomes. Chromosomes 2, 3, 4, and 10 each contained one gene (*PbrBGAL1*, *PbrBGAL2*, *PbrBGAL3*, and *PbrBGAL6*, respectively), whereas chromosomes 9 and 11 contained two genes (*PbrBGAL4/PbrBGAL5* and *PbrBGAL7/PbrBGAL8*, respectively) and chromosome 15 contained four genes (*PbrBGAL9*, *PbrBGAL10*, *PbrBGAL11*, and *PbrBGAL12*) (Fig. 3). We also determined that *PbrBGAL* genes were involved in three whole-genome duplication events (involving *PbrBGAL11* and *PbrBGAL1*, *PbrBGAL11* and *PbrBGAL5*, and *PbrBGAL2* and *PbrBGAL8*) and 10 dispersed duplication events (including paired duplications involving *PbrBGAL3*, –6, –7, and –10;

duplications involving *PbrBGAL4* and *PbrBGAL2*, –8, –9, and –12). Hence, the latter was the main duplication event (Fig. 3).

To clarify the differences in *PbrBGAL* gene structures in each cluster, we constructed an unrooted phylogenetic tree and analyzed exon/intron structures and motifs. The *PbrBGAL* genes consisted of 1–24 exons and 0–23 introns. Moreover, the exon/intron structure was essentially conserved in all subclasses, with the exception of subclass E (Fig. 4). Five genes (*PbrBGAL2*, –3, –6, –8, and –9) encoded all 15 motifs revealed by MEME, but *PbrBGAL4* encoded only three motifs. Notably, 15 *PbrBGAL* genes encoded motif 8 comprising G-G-P-[LIVM](2)-x(2)-Q-x-E-N-E-[FY]. Similar to the exon/intron structure, similar motifs were detected in all subclasses, except for subclass E (Fig. 4).

Identification of PbrBGAL genes involved in pear PTG

We performed a qPCR analysis of the relative expression levels of 12 *PbrBGAL* genes in 14 pear samples. Only *PbrBGAL6* and *PbrBGAL7* were highly expressed in pollen tubes. Interestingly, *PbrBGAL6* was highly expressed specifically in the anther and pollen, but its expression level tended to decrease during PTG, suggestive of a relationship with PTG (Fig. 5). In addition, *PbrBGAL2*, –7, –8, and –9 transcripts accumulated to relatively high levels in the style. *PbrBGAL1*, –3, and –4 were highly expressed in petals, while *PbrBGAL5*, –10, and –11 were highly expressed in leaves (Fig. 5). Both *PbrBGAL3* and *PbrBGAL12* were expressed at relatively low levels in the examined tissues (Fig. 5).

Functional analysis of PbrBGAL6

To assess the potential role of *PbrBGAL6* during PTG, we first screened primers for an as-ODN experiment. The results indicated that as-ODN4 and as-ODN5 treatments significantly enhanced PTG, with the effects of the latter reaching an extremely significant level (Fig. 6A). Therefore, *PbrBGAL6* expression and BGAL enzymatic activity was significantly suppressed in pollen tubes treated with as-ODN5 (as-ODN) (approximately 1.28-fold and 3.2-fold lower than it in the control and s-ODN-treated pollen tubes) (Fig. 6B, 6C), which resulted in a significant increase in pollen tube length (approximately 60 μm) (Fig. 6D, 6E) and apical width (approximately 1.77 μm) (Fig. 6F) as well as cytoplasmic leakage during PTG (Fig. 6D). It may be because effective inhibition of *PbrBGAL6* expression affects the apical pectin component to stimulate rapid PTG accompanied by a wide and leaky tip region.



Fig. 1 PbrBGAL amino acid sequence alignment. Solid blue, green, purple, brown, and gray lines represent I, II, III, IV, and C-terminal regions, respectively. Red, faint yellow, cyan, and green shading indicate the GH35 conserved sequence, SCOP domain d1b9za2, GHD domain, and galactose-binding lectin domain, respectively. The sequence in the red box is a signal peptide. Asterisks and triangles indicate enzyme active and functional sites, respectively. Uppercase letters with different colors reflect different similarities (cyan: $\geq 50\%$; magenta: $\geq 75\%$; and black: 100%)

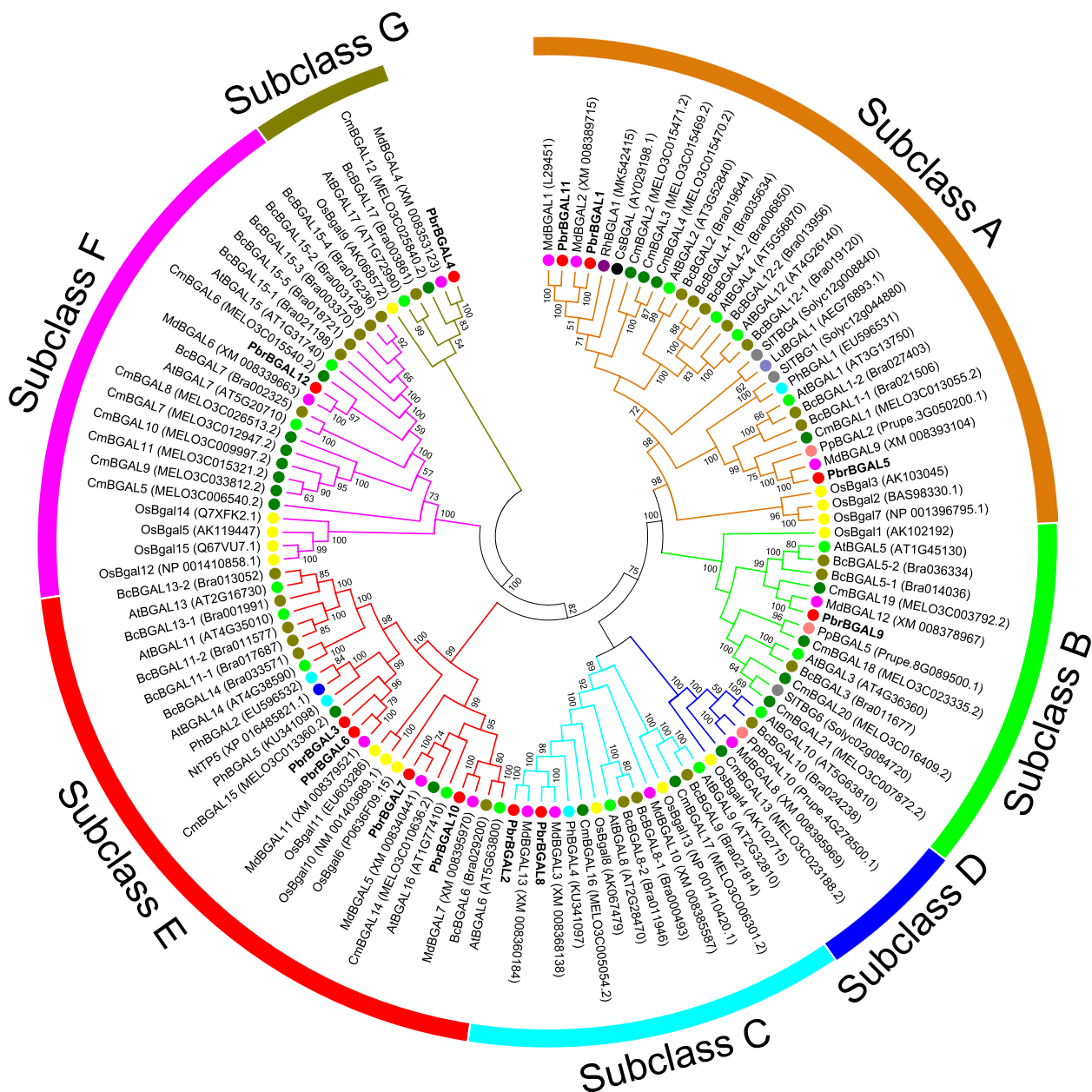


Fig. 2 Phylogenetic tree of BGALs in Chinese white pear and other species. BGALs in twelve species are AtBGALs (*Arabidopsis thaliana*), BcBGALs (*Brassica campestris* ssp. *chinensis*), CmBGALs (*Cucumis melo*), CsBGALs (*Citrus sinensis*), LuBGALs (*Linum usitatissimum*), MdBGALs (*Malus domestica*), NtTP5 (*Nicotiana tabacum*), OsBGALs (*Oryza sativa*), PhBGALs (*Petunia hybrida*), PpBGALs (*Prunus persica*), RhBGALs (*Rosa hybrid cultivar*) and SITBGs (*Solanum lycopersicum*). Differentially colored circular rings and branches represent different subclasses. Differentially colored solid dots indicate BGALs in different species. Bootstrap values less than 50 are not provided in this tree

PbrBGAL6 affects the apical pectin content in the pear pollen tube

To determine the effect of PbrBGAL6 on PTG, we first measured the total pectin content according to ruthenium red staining. The comparison with the control and s-ODN indicated the apical staining of the as-ODN pollen tube was lighter, with a significant decrease in the

average grayscale value (apical 5 μm diameter) (Fig. 7A, 7B). Furthermore, the immunofluorescence of apical methylated pectin was more intense in the as-ODN pollen tube than in the control and s-ODN, which was consistent with the fluorescence intensity (Fig. 7C, 7D). Moreover, inhibited PbrBGAL6 expression clearly decreased the apical ROS content (Fig. 7E, F), but had

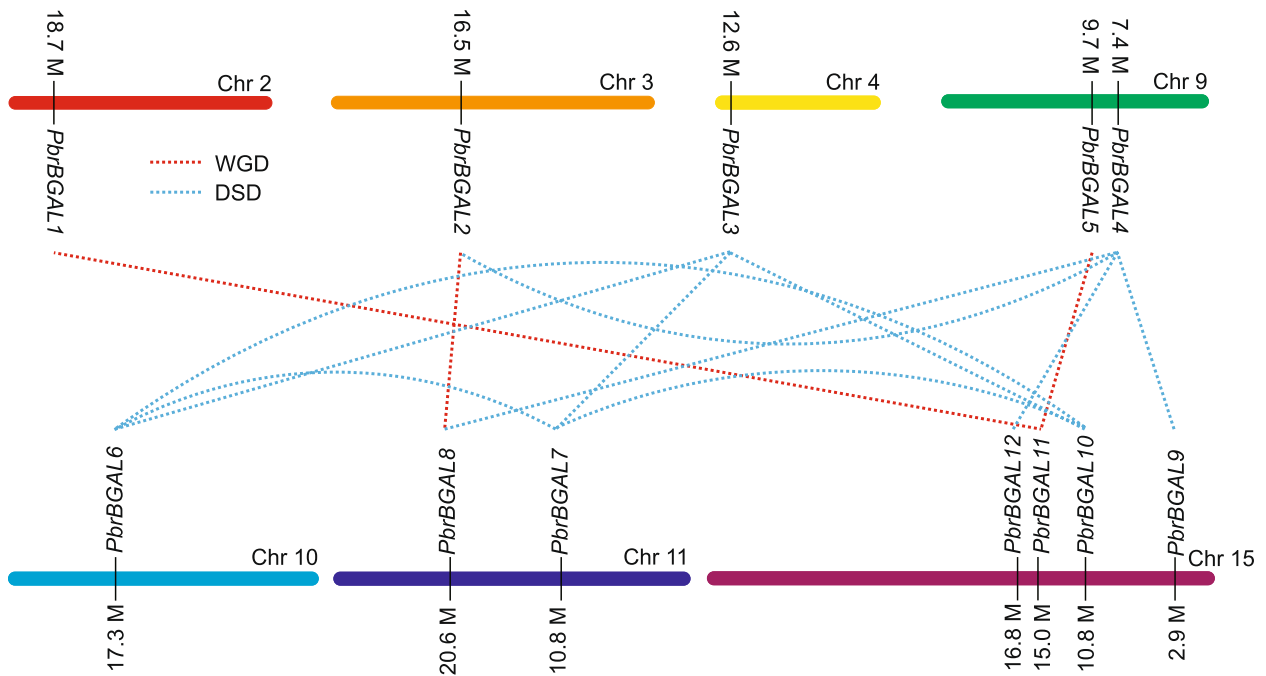


Fig. 3 Chromosomal localization and replication mode of *PbrBGAL* genes. Red and blue dashed lines represent gene pairs derived from whole-genome duplication (WGD) and dispersed duplication (DSD) events, respectively

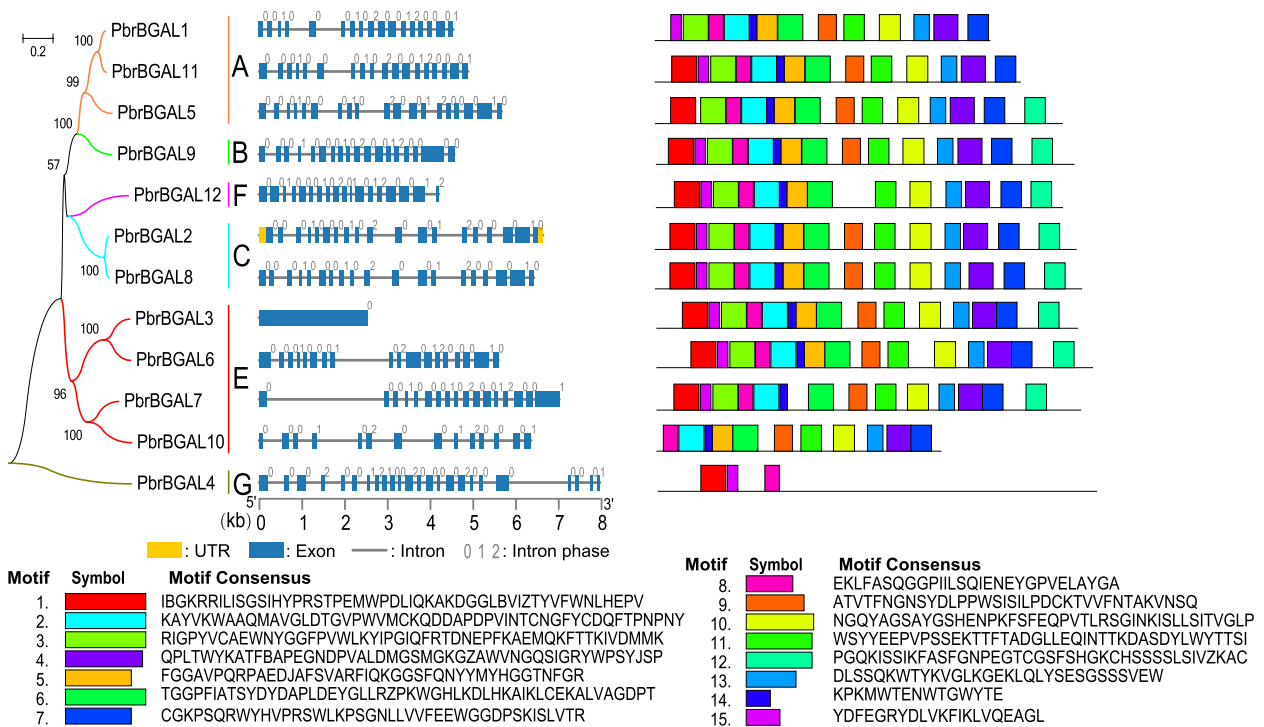


Fig. 4 *PbrBGAL* structures and encoded motifs in each subclass. Left: phylogenetic tree of *PbrBGAL* genes in Chinese white pear, with differentially colored branches representing different subclasses. Middle: *PbrBGAL* intron/exon structures, with Arabic numerals in the top corner indicating the intron phase. Right: motif structures, with each motif consensus sequence provided below the figure

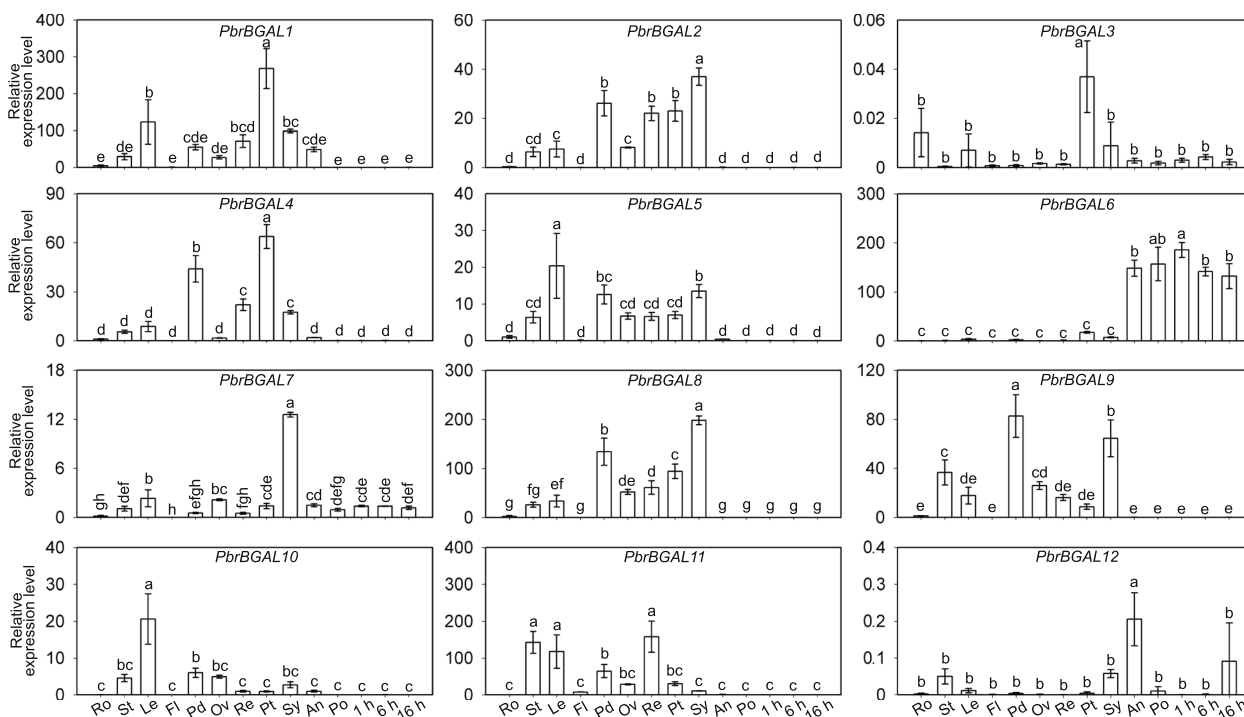


Fig. 5 Tissue-specific expression of 12 *PbrBGAL* genes in 14 different samples. Ro: roots, St: stems, Le: leaves, Fl: flesh, Pd: pedicels, Ov: ovaries, Re: receptacles, Pt: petals, Sy: styles, An: anthers, Po: mature pollen, 1 h: hydrated pollen, 6 h: growing pollen tubes and 16 h: stopped-growth pollen tubes. Data are presented as the mean \pm standard error ($n = 3$ biological replicates). Different lowercase letters indicate significant differences ($P < 0.05$)

little effect on actin cytoskeleton depolymerization (Fig. 7G, 7H).

We also attempted to determine the reasons for apical pectin changes. Of the three PTG-related *PbrPME* genes that were analyzed (*PbrPME11*, -44 , and -59), the *PbrPME11* expression level was higher (approximately 1.8-fold) in the as-ODN pollen tube than in the control and s-ODN [47] (Fig. 8). We also detected the substantial accumulation of *PbrPG14*, -20 , -21 , -22 , -24 , and -33 transcripts in pollen tubes [48, 49], with *PbrPG14* (approximately 1.6-fold), -20 (approximately 1.6-fold), -21 (approximately 1.5-fold), and -24 (approximately 1.7-fold) expression levels that were significantly higher in the as-ODN pollen tubes than in the control and s-ODN (Fig. 8). These results suggest that inhibiting *PbrBGAL6* expression may decrease the apical pectin content because of the associated increases in *PbrPME11* and *PbrPG14*, -20 , -21 , and -24 transcription, thereby temporarily promoting pear PTG.

Discussion

BGALs contribute to pectin modification-related biological processes through their enzymatic activities. In many species, *BGAL* families have been screened to identify key members. *BGAL* genes have been identified in at

least 13 species, including 17 *AtBGAL* genes in *A. thaliana* [31], 15 *OsBgal* genes in rice [32], and 27 *BcBGAL* genes in cabbage [33], 17 *Ibbgals* in sweetpotato [34], 43 *LuBGALs* in flax [35], 51 *GhBGALs* in cotton [36], 21 *CmbGALs* in melon [23], 17 *TBGs* in tomato [37], 13 *Md β -Gals* in apple [43], 8 *PpGALs* in Japanese pear [38], 4 *PaGALs* in avocado [39], 17 *PpBGALs* in peach [40] and 4 *Fa β gals* in strawberry [41, 42]. In the current study, we identified 12 *PbrBGAL* genes in the Chinese white pear genome (Table 1). Interestingly, *BGAL* gene families are relatively small in Rosaceae species, suggestive of limited duplication (especially in Chinese white pear (Fig. 3), in which only whole-genome duplication and dispersed duplication events were detected). The number of *BGAL* genes varied greatly among six Rosaceae fruit tree species, possibly because of differences in species and duplication modes. Hence, *PbrBGAL* genes in Chinese white pear must be comprehensively identified and characterized.

A systematic sequence alignment showed that 12 *PbrBGAL* sequences contained a typical GH35 conserved sequence and two enzyme active sites (E217 and E288) (Fig. 1), which is in accordance with published results for Japanese pear [38], avocado [39], peach [40], and tomato [37]. Thus, these proteins may have GH35 family

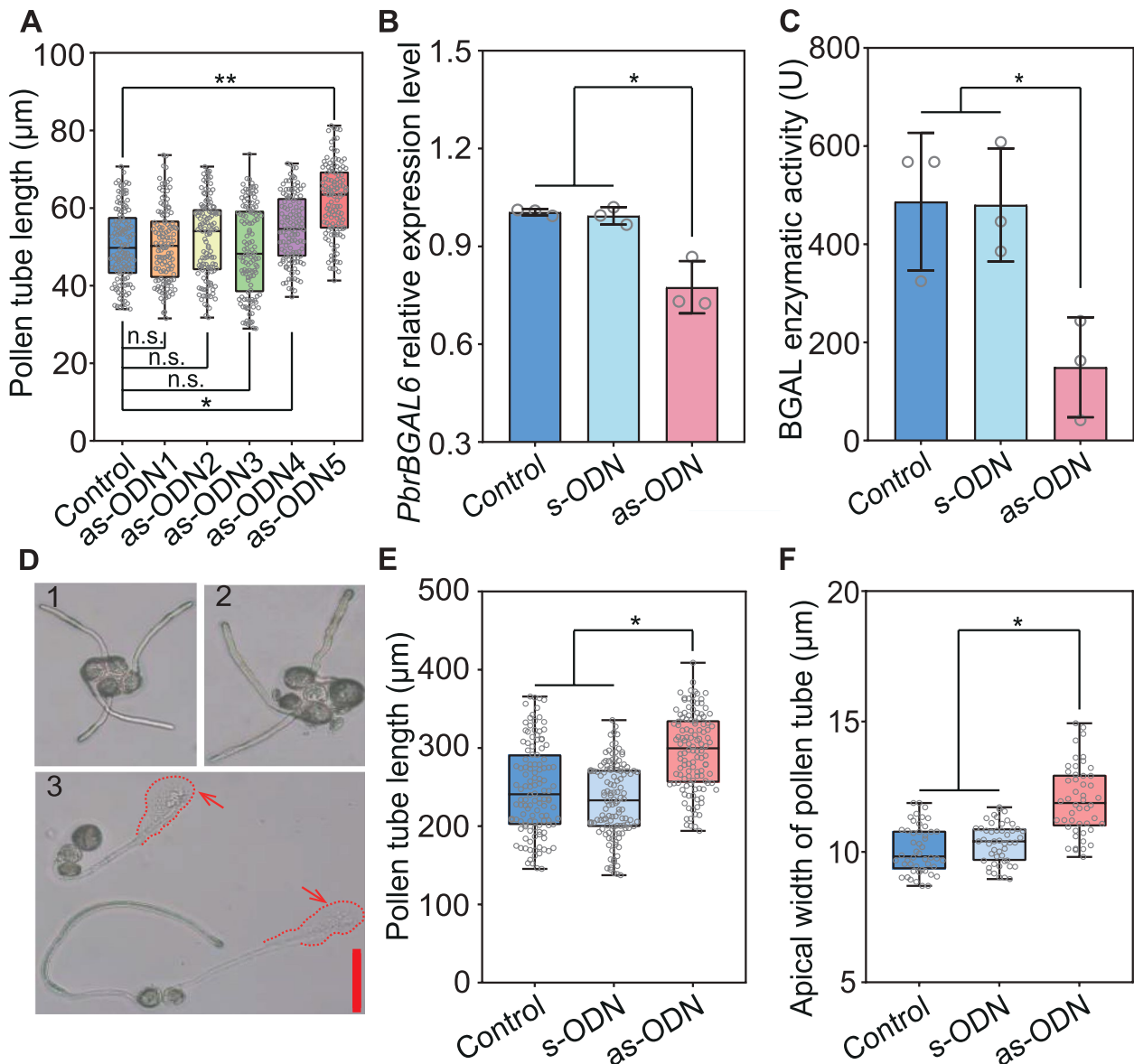


Fig. 6 Inhibited *PbrBGAL6* expression increases the pear pollen tube length, apical width, and cytoplasmic leakage. **A** Effect of five as-ODN primer treatments on the pollen tube length. A total of 120 randomly selected pollen tubes per group were used to measure length. **B** *PbrBGAL6* relative expression level. Data are presented as the mean \pm standard error ($n=3$ biological replicates). **C** BGAL enzymatic activity of pollen tube. Mean \pm standard error ($n=3$ biological replicates) are displayed in column diagram. **D** Representative images of pollen tubes after *PbrBGAL6* expression were suppressed. Arabic numerals represent the control, s-ODN, and as-ODN (1, 2, and 3, respectively). The red irregular dashed line and arrow indicate regions with cytoplasmic leakage and pollen tube leakage, respectively; bar = 100 μm . **E** and **F** Pollen tube length and apical width. A total of 120 and 48 pollen tubes were used to calculate length and width, respectively. Extremely significant ($P < 0.01$), significant ($P < 0.05$), and non-significant differences are indicated by **, *, and n.s., respectively

hydrolytic enzyme activities. However, PpGAL1 and -4 in Japanese pear [38] and AV-GAL1 in avocado [39] lack galactose-binding lectin domain substrates, which is consistent with our findings for *PbrBGAL1*, -10, and -11 (Fig. 1). The same phenomenon was reported for PpBGAL6 and -7 in peach [40] and CmBGAL2, -3, -4, -12, -13, and -16 in melon [23]. These results imply

that *PbrBGALs* may bind to different substrates to perform various functions. The functional sites of tomato TBG4 (N282, N459, and V548; unlabeled in Fig. 1) [37] and *S. pneumoniae* BGAL (W240, W243, and Y455) were not conserved in *PbrBGALs*, which further reflects the functional divergence among *PbrBGALs*. This is likely directly associated with gene duplication [50]. Moreover,

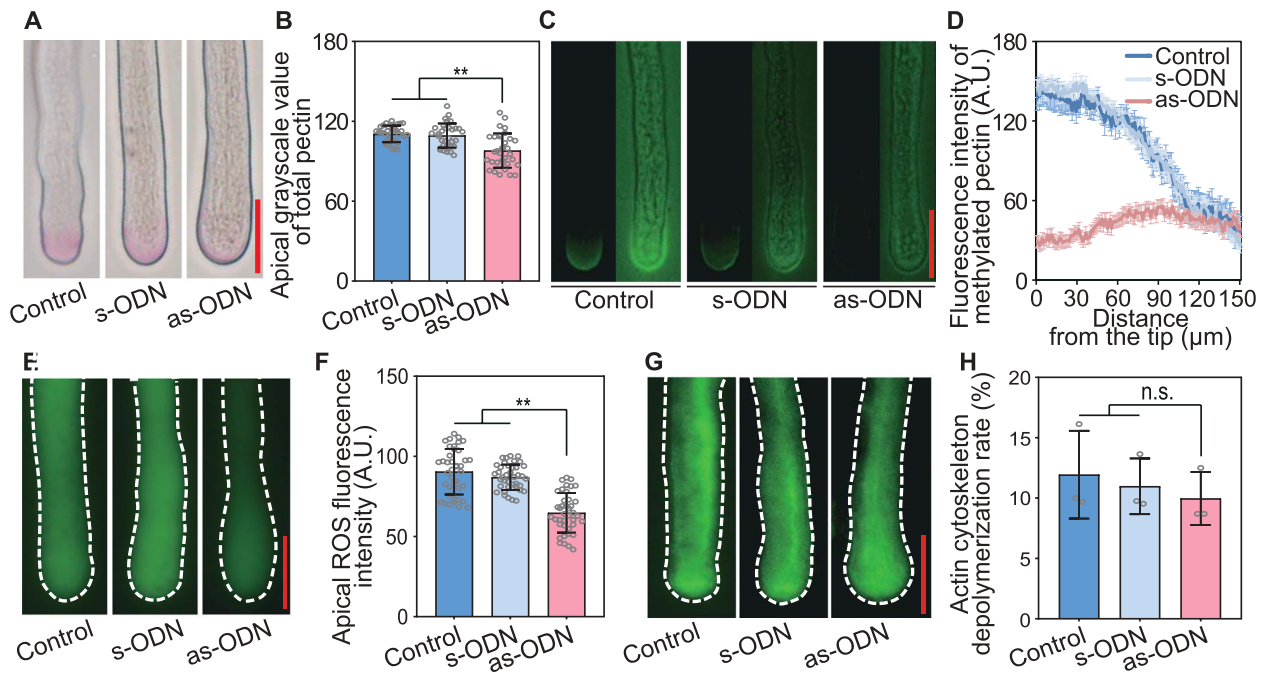


Fig. 7 Inhibited *PbrBGAL6* expression affects apical pectin, total ROS, and actin cytoskeleton in pollen tubes. **A, C, E, and G** Representative images of the total apical pectin, methylated pectin, total ROS, and actin cytoskeleton in control, s-ODN and as-ODN, respectively. **B, D, F, and H** are the quantification of **A, C, E, G**, respectively. **B and F:** Average value of grayscale and fluorescence intensity in a circle within tip 5 μm diameter, respectively. **D:** Fluorescence density from tip to shank on one side of pollen tube. **H:** Average depolymerization rate of actin cytoskeleton. Bar = 20 μm; 30 (**B**), 39 (**D**), 39 (**F**), and 102 (**H**) pollen tubes in each group were analyzed. Extremely significant ($P < 0.01$) and non-significant differences are indicated by ** and n.s., respectively

two other conserved domains (SCOP and GHD) were detected, but their functions will need to be experimentally verified.

A total of 119 *BGAL* genes from 14 species (including Chinese white pear) were classified into seven subclasses (A–G) that differed regarding function. As expected, all subclass E *BGAL* genes were highly expressed in flowers (Fig. 2). According to expression characteristics and earlier research by Pan et al. (2022) [23], we subdivided subclass E into part 1 [from *OsBgal10* (NM 001403689.1) to *BcBGAL13-2* (Bra013052)] and part 2 [from *OsBgal6* (P0636F09.15) to *AtBGAL6* (AT5G63800)] (Fig. 2). Genes in part 1 were mainly specifically expressed in flowers, pollen, and pollen tubes, including *MdBGAL11* (homolog of *PbrBGAL3* and –6) [43], *NTP5* (participates in PTG) [44], *BcBGAL11*, –13, and –14 [33], and *AtBGAL11*, –13, and –14 [37]. Although genes in part 2 were highly expressed in flowers, they were also expressed in other tissues (e.g., stems, leaves, and fruits), including *MdB-GAL5* and –7, *CmBGAL14*, and *BcBGAL6*. Therefore, compared with the part 2 genes *PbrBGAL7* and –10, the part 1 genes *PbrBGAL3* and –6 are more likely to affect pear PTG. These findings may also help to explain the diversity in intron/exon structures and motifs among subclass E *BGAL* genes (Fig. 4). Moreover, subclass A

BGAL genes may primarily contribute to fruit ripening and softening, shedding, and stem and leaf development. For example, *MdBGAL1* and *MdBGAL2*, which are homologs of *PbrBGAL11* and *PbrBGAL1*, are highly expressed during apple fruit ripening and softening [43]. The antisense-based inhibition of tomato *SITBG4* expression can delay fruit softening (40% increase in firmness) [51]. In addition, *RhBGAL1* and *CmBGAL* may be involved in the abscission of flowers and young fruits [52, 53]. *MdBGAL9*, which is homologous to *PbrBGAL5*, is highly expressed in stems and leaves, and probably contributes to their development [43]. Both *AtBGAL2* [37] and *BcBGAL1-2* [33] may have similar functions. Accordingly, *PbrBGAL1*, –5, and –11 in subclass A may influence fruit ripening and softening or stem and leaf development. Similarly, we also deduced that subclasses E, B/C/D, and G may be mainly related to the development of leaves/flowers/fruits, stems/leaves/fruits, and all tissues, respectively. These results suggest that *PbrB-GAL3* and *PbrBGAL6* may regulate pear PTG.

To verify the results of the above-mentioned bioinformatics analysis, we completed a qPCR analysis of the tissue expression patterns of 12 *PbrBGAL* genes. *PbrBGAL6* was abundantly expressed in the anther, pollen, and pollen tube; this gene probably plays a negative regulatory

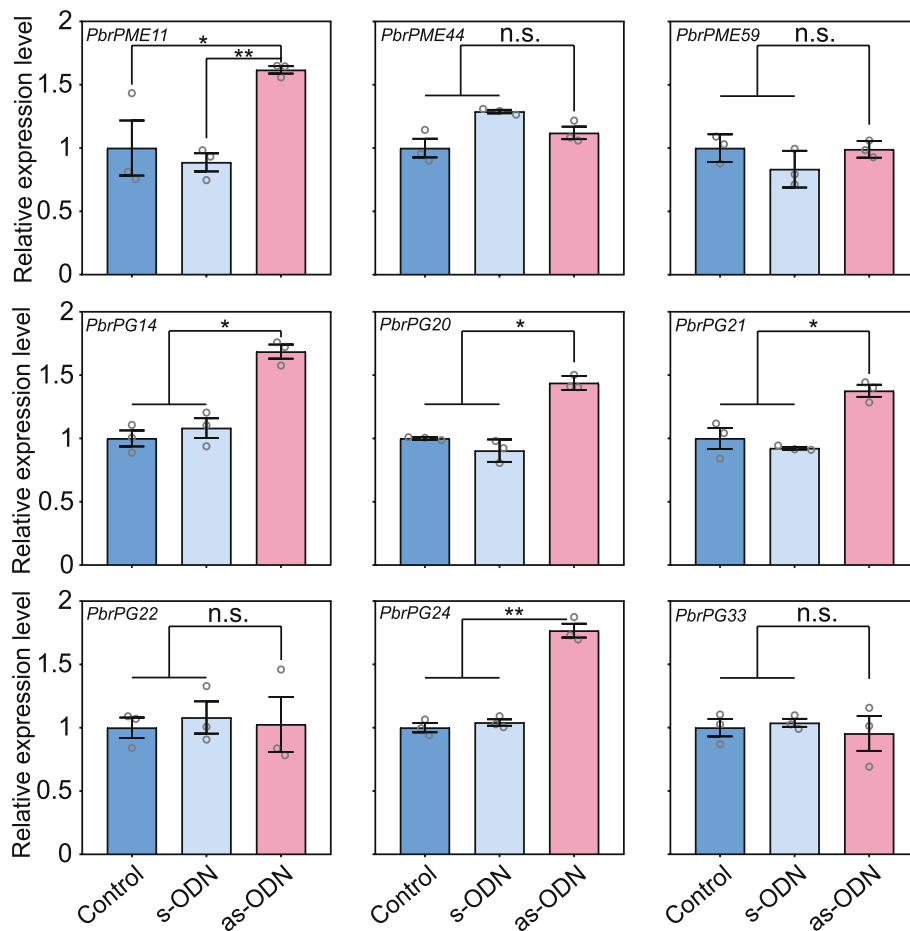


Fig. 8 *PbrPME* and *PbrPG* relative expression levels. Data are presented as the mean \pm standard error ($n = 3$ biological replicates). Extremely significant ($P < 0.01$), significant ($P < 0.05$), and non-significant differences are indicated by **, *, and n.s., respectively

role during PTG (Fig. 5). In other species, more *BGAL* genes are specifically expressed in the stamen. For example, in cotton, *GhBGAL7*, -17, -18, -33, and -43 are specifically expressed in the anther and filament [36]. Similar results were obtained for Chinese cabbage genes *BcBGAL11*, -13, and -15 and rice genes *OsBgal10* and -11 [32, 33]. Moneo-Sánchez et al. (2018) [54] detected relatively few phenotypic changes in β -galactosidase sub-family a1 mutants, indicating that *A. thaliana* *BGAL* genes may have redundant functions [54]. The functional redundancy among these genes may be sufficient for regulating stamen-related processes. However, the functional redundancy of *BGAL* genes may be difficult to assess in pear stamens and pollen tubes because of the substantial transcription of only one gene, suggesting *PbrBGAL6* is probably crucial for pear PTG.

We also observed that inhibiting *PbrBGAL6* expression caused *BGAL* enzymatic activity decrease to rapidly enhance PTG and increase the apical width, which was accompanied by gradual cytoplasm leakage (Fig. 6).

A previous study revealed that *BGALs* can negatively regulate the pectin content to increase cell wall porosity by depolymerizing pectin side-chains involving β -(1,4)/-(1,3)/-(1,6)-glycosidic bonds [23]. This may explain how *PbrBGAL6* contributes to pear pollen tube elongation and leakage. However, our results indicated the total and methylated apical pectin content decreased after *PbrBGAL6* expression was suppressed (Fig. 7 A-D). We previously observed that changes in *PpBGAL10* and *PpBGAL16* expression affect *PpPME3* and *PpPG21* transcription, which influences peach fruit softening [24]. We speculate that in addition to its enzymatic activity, *PbrBGAL6* may also affect the expression of genes encoding pectin-modifying enzymes (*PbrPME* and *PbrPG*) to help regulate the above-mentioned phenotype. Therefore, the expression of the main *PbrPME* genes (*PbrPME11*, *PbrPME44*, and *PbrPME59*) [47] and *PbrPG* genes [49] related to pear PTG were analyzed. The results showed that the transcription of *PbrPME11* (approximately 1.8-fold) and *PbrPG14* (approximately 1.6-fold), -20

(approximately 1.6-fold), *-21* (approximately 1.5-fold), and *-24* (approximately 1.7-fold) increased significantly in control and as-ODN pollen tubes (Fig. 8). PbrPMEs may be associated with an increase in demethylated pectin (hard pectin) and a decrease in the amount of methylated apical pectin (soft pectin). An increase in the hard pectin content can inhibit PTG [18]; however, PbrPGs specifically break the α -(1–4) glycosidic bond of hard pectin, leading to the degradation of HG pectin [19, 20]. Additionally, more *PbrPG* genes (*PbrPG14*, *-20*, *-21*, and *-24*) had increased expression levels than *PbrPME* genes (*PbrPME11*) (Fig. 8), which may ensure that for hard pectin, the degradation rate is greater than the synthesis rate. The PbrBGAL6 may lead to some pectin degradation, ultimately decreasing apical pectin levels in pollen tubes. These results suggest that the PbrBGAL6 enzymatic activity (direct degradation of RG1 pectin) and regulatory effects (indirect degradation of HG pectin via increased PME and PG production) decrease the apical pectin content, leading to transient overgrowth accompanied by cytoplasmic leakage in the pear pollen tube. According to previous speculation [24], the possibility that PbrBGAL6 can produce small sugars (including galactose) by degrading pectin and that sugars act as signaling molecules to promote the synthesis of hormones, such as ethylene [55], or the expression of transcription factor genes (including *SEP1* and *PbrbZIP77*) [16, 56] remains the key to explaining the regulatory effects of PbrBGAL6 on *PbrPME11*, *PbrPG14*, *-20*, *-21*, and *-24* expression. Moreover, ROS may serve as signaling molecules [57], oxidants affecting cell wall cross-linking, and cell wall-loosening compounds [58] to participate in PTG. High ROS concentrations can result in cell wall rigidification that prevents cell expansion [59]. Considering our results, inhibiting *PbrBGAL6* expression can decrease the apical ROS level (Fig. 7E, 7F), suggestive of the loosening of the apical cell wall. Cell wall loosening within a suitable range due to an appropriate decrease in the apical ROS content may promote polar cell growth; however, excessive loosening can cause the cell to rupture, thereby limiting growth [60]. In this study, PbrBGAL6 was revealed to likely influence changes in apical ROS levels within an appropriate range to promote transient PTG. Therefore, the pollen tube phenotype due to inhibited *PbrBGAL6* expression may also be related to the apical ROS content. The relationship between apical ROS and pectin content changes will need to be explored in future investigations.

Conclusions

In summary, we identified 12 *PbrBGAL* genes (*PbrBGAL1–12* divided into six subclasses) in the Chinese white pear genome. Bioinformatics analyses revealed the functional specificity of each *PbrBGAL* subclass, with

PbrBGAL6 in subclass E potentially involved in PTG. The results of an as-ODN assay indicated that PbrBGAL6 can negatively regulate pear PTG, while positively regulating the pollen tube apical pectin content by decreasing the expression of *PbrPME11* and *PbrPG14*, *-20*, *-21*, and *-24*. Our results provide direct evidence of the regulatory effects of BGAL on PTG.

Methods

Bioinformatic analysis

Pear *PbrBGAL* genes were identified using a three-step process. First, AtBGAL and CmBGAL sequences in *A. thaliana* and *C. melo*, respectively, were selected as queries to screen the Pear Genomics Database (<https://peargenome.njau.edu.cn/>) [61]. Second, we searched the Pear Genomics Database using Hidden Markov Model profiles of the Glyco_hydro_35 domain (Accession no. PF01301) [23] from the Pfam database (<https://pfam.xfam.org/>). Third, candidate *PbrBGAL* genes obtained in the first two steps were screened for the presence of the Glyco_hydro_35 domain using the online SMART database (https://smart.embl.de/index_2.cgi). General information regarding *PbrBGAL1–12* was obtained from the Pear Genomics Database, including the gene description, length of the encoded amino acid sequence, and genome position and direction. In addition, the molecular weight/theoretical isoelectric point and signal peptide of each PbrBGAL were predicted using the online software ExPASy (<https://web.expasy.org/protparam/>) and SignalP v3.0 (<https://www.cbs.dtu.dk/services/SignalP/index.php>), respectively. Moreover, PbrBGAL subcellular localizations were determined using the online software Cell-PLoc 2.0 (<http://www.csbio.sjtu.edu.cn/bioinf/Cell-PLoc-2/>). For multiple sequence alignments, DNAMAN6.0 (Lynnon Biosoft, San Ramon, CA, USA) and WebLogo (<https://weblogo.berkeley.edu/logo.cgi>) were used, with default parameters and consensus sequences, respectively. A phylogenetic tree was constructed using MEGA6.0 software. Specifically, a neighbor-joining method with 1,000 bootstrap replicates to evaluate edge support was applied [62]. MapDraw was used to clarify the chromosomal localization of *PbrBGAL* genes [63]. Information regarding the replication of these genes was previously reported by Qiao et al. (2019) [64]. Exon/intron structures and motifs were analyzed using the online programs GSDS (<https://gsds.cbi.pku.edu.cn/>) and MEME, respectively (<https://meme-suite.org/tools/meme>).

Plant materials

Ten different tissues (roots, stems, leaves, fruit flesh, pedicels, ovary, receptacles, petals, styles, and anthers) were obtained from ‘Dangshansuli’ trees growing at the

Fruit Experimental Field of Anhui Science and Technology University and then immediately frozen in liquid nitrogen prior to isolating RNA. Uncracked mature anthers were incubated at 25 ± 1 °C to produce pollen. Dried pollen grains were wrapped in sulfuric acid paper and then stored at -20 °C in a silicone desiccant. Pollen was cultured in pear pollen medium containing 0.4 mM $\text{Ca}(\text{NO}_3)_2$, 1.5 mM H_3BO_3 , 5 mM 2-(N-morpholino) ethanesulfonic acid hydrate, and 292.1 mM sucrose (pH adjusted to 5.8 using NaOH) at 25 °C with shaking (120 rpm). Pollen and pollen tubes were collected by centrifugation (400 g at 25 °C) at four time points during the culture period as described by Zhou et al. (2016) [48]: 0 h (mature pollen), 1 h (hydrated pollen), 6 h (growing pollen tubes), and 16 h (no detectable pollen tube growth). All four samples were quickly stored at -80 °C prior to the subsequent RNA extraction.

Real-time quantitative PCR (qPCR) assays

RNA and cDNA preparation: Total RNA was isolated from each sample using a FastPure Universal Plant Total RNA Isolation Kit (Vazyme, Nanjing, China). RNA quality was assessed by 1.2% agarose gel electrophoresis, whereas RNA integrity was evaluated using a NanoDrop 2000 ultraviolet spectrophotometer (Thermo Fisher Scientific, Waltham, USA). An EasyScript[®] One-Step gDNA Removal and cDNA Synthesis SuperMix kit (TransGen, Beijing, China) was used to reverse transcribe high-quality RNA to cDNA. **Primer preparation:** Gene-specific primers (Additional file 1) were designed using Primer Premier 6.0 (PREMIER Biosoft International, San Francisco, USA) and synthesized (PAGE purification type) by Sangon Biotech (Shanghai) Co., Ltd (Sangon, Shanghai, China). **qPCR assay:** Samples comprising 1 μL 10 μM sense and anti-sense primers, 1 μL 100 ng/ μL cDNA, 2 μL double-distilled H_2O , and 5 μL 2 \times SYBR Premix Ex Taq II (Vazyme) were prepared for a qPCR analysis, which was completed using a LightCycler 480 II system (Roche, Basel, Switzerland) and the following program: 95 °C for 1 min; 40 cycles of 95 °C for 10 s, annealing temperature for 30 s, and 72 °C for 30 s; 40 cycles to construct a melting curve. Relative gene expression levels were calculated according to the $2^{-\Delta\Delta\text{Ct}}$ method [65], with a pear *TUB* gene (*Pbr042345.1*) serving as a reference control. The qPCR assay was repeated at least three times.

Antisense oligodeoxynucleotide (as-ODN) assays

A published procedure that was modified slightly was used to complete as-ODN assays (Chen et al. 2018) [66]. **Primer preparation:** *PbrBGAL6* as-ODN primers were designed using the RNAfold web server (<https://rna.tbi.univie.ac.at/cgi-bin/RNAWebSuite/RNAfold.cgi>). Candidates were screened by evaluating their match to target

regions using Snap Gene 2.4.3 (<https://www.snapgene.com>). Target primers for as-ODNs and the corresponding sense-ODNs (s-ODNs) were synthesized using phosphorothioate oligos that were purified via high-performance liquid chromatography (Additional file 1). As-ODN assays: ODN primers and a lipofectamine 3000 transfection reagent (Thermo Fisher Scientific) were mixed in the above-mentioned pear pollen culture medium for 15 min at room temperature. The mixture was then co-incubated with pollen tubes (approximately 50 μm) in the culture medium (final ODN primer concentration: 20 μM) for 1.5 h at 25 °C with shaking (120 rpm). After rinsing three times with the culture medium, pollen tubes were examined and photographed using an Olympus IX73 inverted fluorescence microscope (Olympus, Tokyo, Japan). The length and apical width were measured for at least 40 and 16 pollen tubes, respectively, for each replicate of each sample using Image-ProPlus 6.0 software (Media Cybernetics, Rockville, USA). Experiments were repeated three times.

β -galactosidase activity

BGAL activity of pollen tube was determined by β -Galactosidase (β -GAL) Activity Assay Kit (Boxbio, Beijing, China) according to instruction. The pollen tube samples of as-ODN assay were collected (approximately 0.15 g) to crush using pestle in liquid nitrogen. Ground samples were added to 1 ml extraction buffer, and then centrifuged at 15,000 g 4 °C for 20 min. The 50 μL supernatant was orderly mixed with reagent one (200 μL) and reagent two (250 μL) to incubate for 30 min at 37 °C. Next, the reagent three (1 mL) was added to above mixture, and let it stand at room temperature for 2 min. As BGAL decomposed p-nitrophenyl- β -D-galactopyranoside to p-nitrophenol, which has the maximum absorption at 400 nm, a microplate reader (Thermo Fisher Scientific) was used to measure the absorbance. The production of 1 nmol of p-nitrophenol per gram tissue per hour under 37 °C was defined as one enzyme activity unit (U). Three replicates for each sample.

Detection of pectin at the pear pollen tube apex

Total apical pectin was stained using ruthenium red as previously described [67]. Briefly, 0.05% ruthenium red (Coolaber, Beijing, China) (final concentration) was added to the above-mentioned culture medium containing approximately 50 μm pollen tubes for a 1-h co-incubation at 25 °C with shaking (120 rpm). Pollen tubes were washed three times with culture medium, after which they were examined and photographed using an Olympus IX73 inverted fluorescence microscope (Olympus). Image-ProPlus 6.0 software (Media Cybernetics) was used to calculate the apical grayscale value.

Immunofluorescence technology was used to detect methylated pectin as described by Tang et al. (2023) [16]. Treated pollen tubes were fixed in 4% paraformaldehyde at 25 °C for at least 30 min, after which they were rinsed three times with phosphate-buffered saline (PBS) and blocked with 1% BSA for 30 min. They were subsequently washed three times with 0.1% BSA and then incubated with 0.1% diluted LM20 polyclonal antibody (1:10) overnight. Next, pollen tubes were rinsed three times with 0.1% BSA and then mixed with 0.1% diluted FITC (goat anti-rat; 1:50) for at least 45 min. Pollen tubes were examined using an Olympus IX73 inverted fluorescence microscope (Olympus). ZEN software (Zeiss, Oberkochen, Germany) was used to analyze the fluorescence intensity on one side extending from the tip to the shank along the cell wall.

Staining of total apical ROS and the actin cytoskeleton in pear pollen tubes

The apical ROS content of pollen tubes was determined using CM-H₂DCFDA (20 μM final concentration) [62]. Pollen tubes after the as-ODN experiment were immediately washed with culture medium and then co-incubated with CM-H₂DCFDA for 20 min at 25 °C in darkness. Pollen tubes were rinsed with culture medium at least three times and then examined using an Olympus IX73 inverted fluorescence microscope (Olympus).

The actin cytoskeleton was examined as described by Chen et al. (2018) [66]. Pollen tubes were fixed and rinsed following a three-step process as described for the immunofluorescence assay. Pollen tubes were permeabilized using 0.5% Triton X-100 at 25 °C for 10 min. After washing three times with PBS, the actin cytoskeleton was stained using 1% phalloidin for 20 min at 25 °C and then examined using an Olympus IX73 inverted fluorescence microscope (Olympus). The average apical fluorescence density of ROS and the actin cytoskeleton in a region with a 5 μm diameter was measured using ZEN software. The experiment was repeated three times.

Statistical analysis

GraphPad Prism 8.0.1 (GraphPad, San Diego, USA) was used to generate figures presenting mean values and standard errors. Post hoc Tukey's tests for a one-way ANOVA ($P < 0.05$) and Student's *t*-test ($P < 0.05$) were completed using IBM SPSS Statistics 22 software (IBM, Armonk, USA) to determine the significance of differences between multiple samples and between two samples, respectively.

Abbreviations

BGAL	β-Galactosidase
SI	Self incompatibility
PTG	Pollen tube growth

GH35	Glycosyl hydrolase 35
Chr	Chromosome
Mw	Molecular weight
pl	Theoretical isoelectric point
WDG	Whole-genome duplication
DSD	Dispersed duplication
PME	Pectin methyltransferase
PG	Polygalacturonase
HG	Homogalacturonan
RG-I	Rhamnogalacturonan I
RG-II	Rhamnogalacturonan II
PAE	Pectin acetyltransferase
PL	Pectate lyases
PMEI	PME inhibitor
qPCR	Real-time quantitative PCR
as-ODN	Antisense oligodeoxynucleotide
s-ODN	Sense oligodeoxynucleotide
PBS	Phosphate buffer solution
BSA	Bovine serum albumin
FITC	Fluorescein isothiocyanate
ROS	Reactive oxygen species

Supplementary Information

The online version contains supplementary material available at <https://doi.org/10.1186/s12864-025-11429-9>.

Supplementary Material 1.

Supplementary Material 2.

Acknowledgements

We thank Xiaomin Lu for editing the English text of a draft of this manuscript.

Authors' contributions

YX, SJ, GC and MQ designed the experiments. YX, LX, MZ, HW and YW took all pear samples. YX, LX, MQ, YW, HW and XZ performed all the molecular biology experiments. YX, KZ, YS, JQ and MQ performed bioinformatics analysis. YX, LX, MZ and MQ analyzed all the data. YX, MQ and GC wrote the manuscript. YX and MQ revised the whole manuscript.

Funding

This study was supported by grants from Youth Fund of the National Natural Science Foundation of China (Grant number 32302615), Natural Science Research Project of Anhui Educational Committee, China (Grant number 2022AH051616), and College Students' Innovative Entrepreneurial Training Plan Program, China (Grant number S202310879169).

Data availability

The datasets analyzed during the current study are available in the Pear Genome Project, CuGenDB, GenBank and TAIR repository, the gene accession numbers of *Pyrus bretschneideri* from Pear Genome Project (<https://peargenome.njau.edu.cn/>) are shown in Table 1, The gene accession numbers of *Arabidopsis thaliana* from TAIR (<http://www.arabidopsis.org/>), of *Solanum lycopersicum* and *Prunus persica* from Phytozome v13 (<https://phytozome.jgi.doe.gov/>), of *Cucumis melo* from CuGenDB (<http://cucurbitgenomics.org/>), of *Brassica campestris ssp. chinensis*, *Citrus sinensis*, *Linum usitatissimum*, *Malus domestica*, *Nicotiana tabacum*, *Oryza sativa*, *Petunia hybrida* and *Rosa hybrid cultivar* from GenBank (<https://www.ncbi.nlm.nih.gov/genbank/>) respectively are shown in Additional file 2.

Declarations

Ethics approval and consent to participate

All experimental studies on plants were complied with relevant institutional, national, and international guidelines and legislation.

Consent for publication

Not applicable.

Competing interests

The authors declare no competing interests.

Received: 16 August 2024 Accepted: 3 March 2025

Published online: 31 March 2025

References

- Zhang D, Li Y, Zhao X, Zhang C, Liu D, Lan S, et al. Molecular insights into self-incompatibility systems: from evolution to breeding. *Plant Commun.* 2024;5(2):100719.
- Wu L, Liu X, Zhang M, Qi K, Jiang X, Yao J, et al. Self S-RNase inhibits ABF-LRX signaling to arrest pollen tube growth to achieve self-incompatibility in pear. *Plant J.* 2023;113(3):595–609.
- Hepler P, Rounds C, Winship L. Control of cell wall extensibility during pollen tube growth. *Mol Plant.* 2013;6(4):998–1017.
- Cascallares M, Setzes N, Marchetti F, López G, Distéfano A, Cainzos M, et al. A complex journey: cell wall remodeling, interactions, and integrity during pollen tube growth. *Front Plant Sci.* 2020;11:599247.
- Chebli Y, Kaneda M, Zerkour R, Geitmann A. The cell wall of the Arabidopsis pollen tube-spatial distribution, recycling, and network formation of polysaccharides. *Plant Physiol.* 2012;160(4):1940–55.
- Roggen H, Stanley R. Autoradiographic studies of pear pollen tube walls. *Physiol Plant.* 2010;24(1):80–4.
- Li X, Tang C, Li X, Zhu X, Cai Y, Wang P, et al. Cellulose accumulation mediated by PbrCSLD5, a cellulose synthase-like protein, results in cessation of pollen tube growth in *Pyrus bretschneideri*. *Physiol Plant.* 2022;174(3):e13700.
- Wang W, Wang L, Chen C, Xiong G, Tan X, Yang K, et al. *Arabidopsis CSLD1* and *CSLD4* are required for cellulose deposition and normal growth of pollen tubes. *J Exp Bot.* 2011;62(14):5161–77.
- Cao P, Tang C, Wu X, Qian M, Lv S, Gao H, et al. PbrCalS5, a callose synthase protein, is involved in pollen tube growth in *Pyrus bretschneideri*. *Planta.* 2022;256(2):22.
- Cai G, Faleri C, Casino C, Emons A, Cresti M. Distribution of Callose Synthase, Cellulose Synthase, and Sucrose Synthase in Tobacco Pollen Tube Is Controlled in Dissimilar Ways by Actin Filaments and Microtubules. *Plant Physiol.* 2011;155(3):1169–90.
- Kotake T, Li Y, Takahashi M, Sakurai N. Characterization and function of wall-bound exo- β -glucanases of *Lilium longiflorum* pollen tubes. *Sex Plant Reprod.* 2000;13(1):1–9.
- Shoseyov O, Dekel-Reichenbach M. The role of endo-1,4-beta-glucanase in plant cell elongation. in-vitro studies of peach pollen. *Acta Horticulturae.* 1993;1993(329):225–27.
- Kamel H, Geitmann A. Strength in numbers: An isoform variety of homogalacturonan modifying enzymes may contribute to pollen tube fitness. *Plant Physiol.* 2023;194(1):67–80.
- Dumont M, Lehner A, Bouton S, Kiefer-Meyer M, Voxeur A, Pelloux J, et al. The cell wall pectic polymer rhamnogalacturonan-II is required for proper pollen tube elongation: implications of a putative sialyltransferase-like protein. *Ann Bot.* 2014;114(6):1177–88.
- Dardelle F, Lehner A, Ramdani Y, Bardor M, Lerouge P, Driouch A, et al. Biochemical and immunocytological characterizations of Arabidopsis pollen tube cell wall. *Plant Physiol.* 2010;153(4):1563–76.
- Tang C, Wang P, Zhu X, Qi K, Xie Z, Zhang H, et al. Acetylation of inorganic pyrophosphatase by S-RNase signaling induces pollen tube tip swelling by repressing pectin methylesterase. *Plant Cell.* 2023;35(9):3544–65.
- Willats W, Orfila C, Limberg G, Buchholt H, Alebeek G, Voragen A, et al. Modulation of the Degree and Pattern of Methyl-esterification of Pectic Homogalacturonan in Plant Cell Walls: IMPLICATIONS FOR PECTIN METHYL ESTERASE ACTION, MATRIX PROPERTIES, AND CELL ADHESION. *J Biol Chem.* 2001;276(22):19404–13.
- Bosch M, Cheung A, Hepler P. Pectin Methylesterase, a Regulator of Pollen Tube Growth. *Plant Physiol.* 2005;138(3):1334–46.
- Hocq L, Guinand S, Habrylo O, Voxeur A, Tabi W, Safran J, et al. The exogenous application of AtPGLR, an endo-polygalacturonase, triggers pollen tube burst and repair. *Plant J.* 2020;103(2):617–33.
- Safran J, Tabi W, Ung V, Lemaire A, Habrylo O, Bouckaert J, et al. Plant polygalacturonase structures specify enzyme dynamics and processivities to fine-tune cell wall pectins. *Plant Cell.* 2023;35(8):3073–91.
- Zhu X, Tang C, Li Q, Qiao X, Li X, Cai Y, et al. Characterization of the pectin methylesterase inhibitor gene family in Rosaceae and role of *PbrP-MEI23/39/41* in methylesterified pectin distribution in pear pollen tube. *Planta.* 2021;253(6):118.
- Sørensen S, Pauly M, Bush M, Skjød M, McCann M, Borkhardt B, et al. Pectin engineering: modification of potato pectin by *in vivo* expression of an endo-1,4- β -D-galactanase. *Proc Natl Acad Sci USA.* 2000;97(13):7639–44.
- Pan H, Sun Y, Qiao M, Qi H. Beta-galactosidase gene family genome-wide identification and expression analysis of members related to fruit softening in melon (*Cucumis melo* L.). *BMC Genomics.* 2022;23(1):795.
- Liu H, Qian M, Song C, Li J, Zhao C, Li G, et al. Down-Regulation of *PpBGAL10* and *PpBGAL16* Delays Fruit Softening in Peach by Reducing Polygalacturonase and Pectin Methylesterase Activity. *Front Plant Sci.* 2018;9:1015.
- Gerardi C, Blando F, Santino A. Purification and chemical characterization of a cell wall-associated β -galactosidase from mature sweet cherry (*Prunus avium* L.) fruit. *Plant Physiol Biochem.* 2012;61:123–30.
- Ross G, Redgwell R, Macrae E. Kiwifruit β -galactosidase: Isolation and activity against specific fruit cell-wall polysaccharides. *Planta.* 1993;189:499–506.
- Ali Z, Armugam S, Lazan H. β -Galactosidase and its significance in ripening mango fruit. *Phytochemistry.* 1995;38(5):1109–14.
- Kotake T, Dina S, Konishi T, Kaneko S, Igarashi K, Samejima M, et al. Molecular Cloning of a β -Galactosidase from Radish That Specifically Hydrolyzes β -(1–3)- and β -(1–6)-Galactosyl Residues of Arabinogalactan Protein. *Plant Physiol.* 2005;138(3):1563–76.
- Hirano Y, Tsumuraya Y, Hashimoto Y. Characterization of spinach leaf α -L-arabinofuranosidases and β -galactosidases and their synergistic action on an endogenous arabinogalactan-protein. *Physiol Plant.* 2010;92(2):286–96.
- Nibbering P, Petersen B, Motawia M, Jørgensen B, Ulvskov P, Niittylä T. Golgi-localized exo- β 1,3-galactosidases involved in cell expansion and root growth in *Arabidopsis*. *J Biol Chem.* 2020;295(31):10581–92.
- Ahn Y, Zheng M, Bevan D, Esen A, Shiu S, Benson J, et al. Functional genomic analysis of *Arabidopsis thaliana* glycoside hydrolase family 35. *Phytochemistry.* 2007;68(11):1510–20.
- Tanhanuch W, Chantarangsee M, Maneesin J, KetudatCairns J. Genomic and expression analysis of glycosyl hydrolase family 35 genes from rice (*Oryza sativa* L.). *BMC Plant Biol.* 2008;8:84.
- Liu J, Gao M, Lv M, Cao J. Structure, Evolution, and Expression of the β -Galactosidase Gene Family in *Brassica campestris* ssp. *chinensis*. *Plant Mol Biol Rep.* 2013;31(6):1249–60.
- Hou F, Du T, Qin Z, Xu T, Li A, Dong S, et al. Genome-wide in silico identification and expression analysis of beta-galactosidase family members in sweetpotato [*Ipomoea batatas* (L.) Lam]. *BMC Genomics.* 2021;22(1):140.
- Hobson N, Deyholos M. Genomic and expression analysis of the flax (*Linum usitatissimum*) family of glycosyl hydrolase 35 genes. *BMC Genomics.* 2013;14:344.
- Cao X, Zhang C, Gou H, Wang X, Qiao K, Ma Q, et al. Genome-wide identification and analysis of β -galactosidase (BGAL) gene family in cotton. *Molecular Plant Breeding.* 2021;12(27):1–16.
- Chandrasekar B, Hoorn R. Beta galactosidases in Arabidopsis and tomato - a mini review. *Biochem Soc Trans.* 2016;44(1):150–8.
- Nagashima A, Mathooko F, Mwaniki M, Kubo Y, Inaba A, Yamaki S, et al. Differential Expression of Members of the β -Galactosidase Gene Family during Japanese Pear (*pyrus pyrifolia* L.) Fruit Growth and On-tree Ripening. *J Amer Soc Hort Sci.* 2005;130(6):819–29.
- Tateishi A, Shiba H, Ogihara J, Isobe K, Nomura K, Watanabe K, et al. Differential expression and ethylene regulation of β -galactosidase genes and isozymes isolated from avocado (*persea americana* Mill.) fruit. *Postharvest Biol Tec.* 2007;45(1):56–65.
- Guo S, Song J, Zhang B, Jiang H, Ma R, Yu M. Genome-wide identification and expression analysis of beta-galactosidase family members during fruit softening of peach (*Prunus persica* (L.) Batsch). *Postharvest Biol Tec.* 2018;136:111–23.
- Trainotti L, Spinello R, Piovan A, Spolaore S, Casadoro G. β -Galactosidases with a lectin-like domain are expressed in strawberry. *J Exp Bot.* 2001;52(361):1635–45.

42. Paniagua C, Blanco-Portales R, Barceló-Muñoz M, García-Gago J, Waldron K, Quesada M, et al. Antisense down-regulation of the strawberry β -galactosidase gene *Fa β Gal4* increases cell wall galactose levels and reduces fruit softening. *J Exp Bot*. 2016;67(3):619–31.
43. Yang H, Liu J, Dang M, Zhang B, Li H, Meng R, et al. Analysis of β -Galactosidase During Fruit Development and Ripening in Two Different Texture Types of Apple Cultivars. *Front Plant Sci*. 2018;9:539.
44. Rogers H, Maund S, Johnson L. A β -galactosidase-like gene is expressed during tobacco pollen development. *J Exp Bot*. 2001;52(354):67–75.
45. Eda M, Matsumoto T, Ishimaru M, Tada T. Structural and functional analysis of tomato β -galactosidase 4: insight into the substrate specificity of the fruit softening-related enzyme. *Plant J*. 2016;86(4):300–7.
46. Cheng W, Wang L, Jiang Y, Bai X, Chu J, Li Q, et al. Structural insights into the Substrate Specificity of *Streptococcus pneumoniae* β (1,3)-Galactosidase BgaC. *J Biol Chem*. 2012;287(27):22910–8.
47. Tang C, Zhu X, Qiao X, Gao H, Li Q, Wang P, et al. Characterization of the pectin methyl-esterase gene family and its function in controlling pollen tube growth in pear (*Pyrus bretschneideri*). *Genomics*. 2020;112(3):2467–77.
48. Zhou H, Yin H, Chen J, Liu X, Gao Y, Wu J, et al. Gene-expression profile of developing pollen tube of *Pyrus bretschneideri*. *Gene Expr Patterns*. 2016;20(1):11–21.
49. Zhang S, Ma M, Zhang H, Zhang S, Qian M, Zhang Z, et al. Genome-wide analysis of polygalacturonase gene family from pear genome and identification of the member involved in pear softening. *BMC Plant Biol*. 2019;19(1):587.
50. Wang M, Yuan D, Gao W, Li Y, Tan J, Zhang X. A Comparative Genome Analysis of PME and PME1 Families Reveals the Evolution of Pectin Metabolism in Plant Cell Walls. *PLoS ONE*. 2013;8(8):e72082.
51. Smith D, Abbott J, Gross K. Down-Regulation of Tomato β -Galactosidase 4 Results in Decreased Fruit Softening. *Plant Physiol*. 2002;129(4):1755–62.
52. Gao Y, Liu Y, Liang Y, Lu J, Jiang C, Fei Z, et al. *Rosa hybrida* RHERF1 and RHERF4 mediate ethylene- and auxin-regulated petal abscission by influencing pectin degradation. *Plant J*. 2019;99(6):1159–71.
53. Wu Z, Burns J. A β -galactosidase gene is expressed during mature fruit abscission of 'Valencia' orange (*Citrus sinensis*). *J Exp Bot*. 2004;55(402):1483–90.
54. Moneo-Sánchez M, Izquierdo L, Martín I, Hernández-Nistal J, Albornos L, Dopico B, et al. Knockout mutants of *Arabidopsis thaliana* β -galactosidase. Modifications in the cell wall saccharides and enzymatic activities. *Biologia Plantarum*. 2018;62(1):80–8.
55. Kim J, Gross K, Solomos T. Characterization of the Stimulation of Ethylene Production by Galactose in Tomato (*Lycopersicon esculentum* Mill.). *Plant Physiol*. 1987;85(3):804–7.
56. Li J, Li F, Qian M, Han M, Liu H, Zhang D, et al. Characteristics and regulatory pathway of the *PrupeSEP1 SEPALLATA* gene during ripening and softening in peach fruits. *Plant Sci*. 2017;257:63–73.
57. Kou X, Sun J, Wang P, Wang D, Cao P, Lin J, et al. PbrRALF2-elicited reactive oxygen species signaling is mediated by the PbrCrRLK1L13-PbrMPK18 module in pear pollen tubes. *Hortic Res*. 2021;8(1):222.
58. Kärkönen A, Kuchitsu K. Reactive oxygen species in cell wall metabolism and development in plants. *Phytochemistry*. 2015;112:22–32.
59. Monshausen G, Bibikova T, Messerli M, Shi C, Gilroy S. Oscillations in extracellular pH and reactive oxygen species modulate tip growth of *Arabidopsis* root hairs. *Proc Natl Acad Sci USA*. 2007;104(52):20996–1001.
60. Mangano S, Juárez S, Estevez J. ROS Regulation of Polar Growth in Plant Cells. *Plant Physiol*. 2016;171(3):1593–605.
61. Wu J, Wang Z, Shi Z, Zhang S, Ming R, Zhu S, et al. The genome of the pear (*Pyrus bretschneideri* Rehd.). *Genome Res*. 2013;23(2):396–408.
62. Qian M, Xu L, Tang C, Zhang H, Gao H, Cao P, et al. *PbrPOE21* inhibits pear pollen tube growth in vitro by altering apical reactive oxygen species content. *Planta*. 2020;252(3):43.
63. Liu R, Meng J. MapDraw: a microsoft excel macro for drawing genetic linkage maps based on given genetic linkage data. *Yi Chuan*. 2003;25(3):317–21.
64. Qiao X, Li Q, Yin H, Qi K, Li L, Wang R, et al. Gene duplication and evolution in recurring polyploidization-diploidization cycles in plants. *Genome Biol*. 2019;20(1):38.
65. Livak K, Schmittgen T. Analysis of Relative Gene Expression Data Using Real-Time Quantitative PCR and the $2^{-\Delta\Delta Ct}$ Method. *Methods*. 2001;25:402–8.
66. Chen J, Wang P, de Graaf B, Zhang H, Jiao H, Tang C, et al. Phosphatidic Acid Counteracts S-RNase Signaling in Pollen by Stabilizing the Actin Cytoskeleton. *Plant Cell*. 2018;30(5):1023–39.
67. Iwai H, Hokura A, Oishi M, Chida H, Ishii T, Sakai S, et al. The gene responsible for borate cross-linking of pectin Rhamnogalacturonan-II is required for plant reproductive tissue development and fertilization. *Proc Natl Acad Sci USA*. 2006;103(44):16592–7.

Publisher's Note

Springer Nature remains neutral with regard to jurisdictional claims in published maps and institutional affiliations.